Quantum stirring of particles in closed devices

Gilad Rosenberg and Doron Cohen

Department of Physics, Ben-Gurion University, Beer-Sheva 84105, Israel

Abstract
We study the quantum analogue of stirring of water inside a cup using a spoon.
This can be regarded as a prototype example for quantum pumping in closed
devices. The current in the device is induced by translating a scatterer. Its
calculation is done using the Kubo formula approach. The transported charge
is expressed as a line integral that encircles chains of Dirac monopoles. For
simple systems, the results turn out to be counter-intuitive, e.g. as we move
a small scatterer 'forward' the current is induced 'backwards'. One should
realize that the route towards quantum-classical correspondence has to do with
'quantum chaos' considerations, and hence assumes greater complexity of the
device. We also point out the relation to the familiar S-matrix formalism which
is used to analyse quantum pumping in open geometries.

PACS numbers: 03.65.−w, 03.65.Vf, 73.23.−b, 05.45.Mt

(Some figures in this article are in colour only in the electronic version)

1. Introduction

Consider a closed ring that contains particles (figure 1(*a*)). Assume that one wants to create
a current in this ring. If the particles are charged, then one way to do it is by creating an
electromotive force (EMF). This can be induced by varying an Aharonov–Bohm flux Φ, such
that by Faraday's law EMF $= -\dot{\Phi}$. But there is another way to create a current that does not
involve EMF, and hence does not assume charged particles. The idea is to change in time the
scalar potential $V(\boldsymbol{r}; X_1(t), X_2(t))$. Here $\boldsymbol{r}$ is the coordinate of a representative particle in the
ring, while X_1 and X_2 are some control parameters. By making a cycle in the (X_1, X_2) space,
we can push non-zero net charge Q through the system. Thus, an 'ac driving' gives rise to a
'dc' component in the current. This is known in the literature as 'quantum pumping'.

In this paper, we would like to consider a prototype pumping problem, which we call
'quantum stirring'. It is the simplest scheme to create a current with a non-vanishing dc
component. Referring to figure 2 we define X_1 as the location of a scatterer, while X_2 is its
'size'. By 'size' we mean either the cross section or the reflection coefficient. One can regard
the scatterer as a 'piston' or as a 'spoon' with which it is possible to 'push' the particles. A
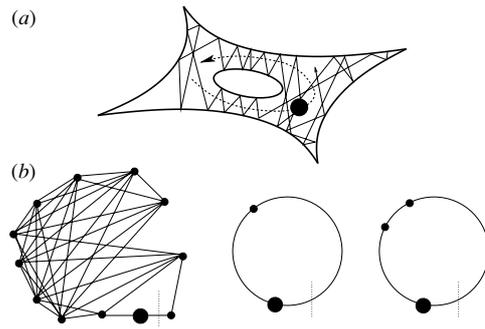
Figure 1. Models for the analysis of quantum stirring. (*a*) A scatterer (big black dot) is translated inside a Sinai billiard. A chaotic trajectory of a representative particle in this billiard is illustrated. (*b*) Network models for quantum stirring. The scatterer (big black dot) is translated along one of the bonds. The vertical dotted line is the section through which the current is measured. From left to right: chaotic network, double barrier model, triple barrier model.
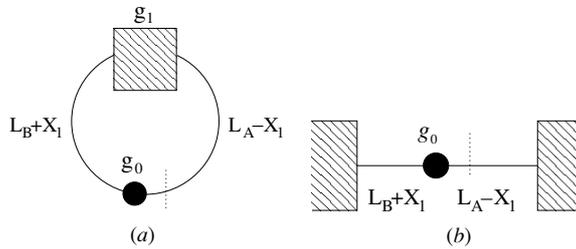

Figure 2. (*a*) A schematic representation of the network model. The vertical dotted line is the section through which the current is measured. The moving scatterer is indicated by its transmission g_0, while X_1 is its displacement along the bond. (*b*) The corresponding open geometry where the left and right leads are connected to reservoirs with the same chemical potentials.
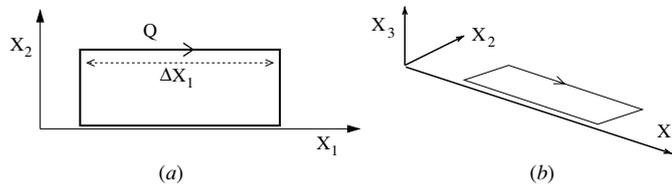
Figure 3. A prototype example for a pumping cycle. During the main stage of the cycle, the scatterer is translated to the right by a distance ΔX_1. Consequently, a charge Q is transported. (*a*) The pumping cycle in the two-dimensional (X_1, X_2) plane. (*b*) The same pumping cycle in the three-dimensional (X_1, X_2, X_3) space, where $X_3 = \Phi$ is the Aharonov–Bohm flux via the ring.

prototype example for a pumping cycle is illustrated in figure 3. During the main stage of the cycle, the scatterer is translated to the right by a distance ΔX_1. Consequently, a charge Q is transported. In the second stage, the size of the scatterer is 'lowered', and it is displaced back to its original location, where its original 'size' is restored. By repeating this cycle many times, we can create a current with a dc component.

In the following analysis, we assume that the system consists of non-interacting spinless particles. All the particles have (formally) charge e, even if they are not actually charged. We assume that there is no magnetic field in the system. Still, for the sake of a later mathematical
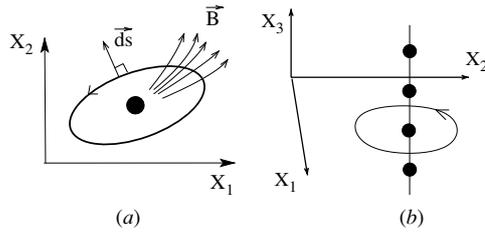
Figure 4. (*a*) The calculation of the charge Q is a line integral over G that can be regarded as a calculation of the flux of $\boldsymbol{B}$ via a two-dimensional curve. $\vec{\mathrm{d}s}$ is a normal vector to the pumping cycle. The black dot in the middle symbolizes the presence of 'magnetic charge' which is characterized by a density $\sigma(X_1, X_2)$. In the quantum-mechanical analysis this should be understood as the density of 'Dirac chains'. (*b*) In the embedding (X_1, X_2, X_3) space, the magnetic charge is organized as vertical charged chains. Each chain consists of 'Dirac monopoles' which are located at $\vec{X}$ points where an occupied level has a degeneracy with a nearby level. The ellipse represents a possible pumping cycle that may encircle either one or many chains.

formulation, it is convenient to introduce a third parameter $X_3 = \Phi$, where Φ is an Aharonov–Bohm flux. The pumping cycle in the (X_1, X_2, X_3) space is illustrated in figure 3.

1.1. Linear response theory and the Dirac chains' picture

We are going to analyse the stirring problem within the framework of linear response theory. If we have EMF then we expect to get in the dc limit Ohm's law $\mathcal{I} = -G\dot{\Phi}$, while if we change slowly either X_1 or X_2 we expect to get in the dc limit $\mathcal{I} = -G^1\dot{X}_1$ or $\mathcal{I} = -G^2\dot{X}_2$, respectively. So, in general, we can write

$$Q = \oint_{\mathrm{cycle}} I \, \mathrm{d}t = -\oint (G^1 \, \mathrm{d}X_1 + G^2 \, \mathrm{d}X_2) = \oint \boldsymbol{B} \cdot \vec{\mathrm{d}s} = \iint \sigma(X_1, X_2) \, \mathrm{d}X_1 \, \mathrm{d}X_2. \qquad (1)$$

In the second expression, we define the normal vector $\vec{\mathrm{d}s} = (\mathrm{d}X_2, -\mathrm{d}X_1)$ and use the notation $\boldsymbol{B}_1 = -G^2$ and $\boldsymbol{B}_2 = G^1$. See figure 4(*a*) for an illustration. The third expression is obtained via the two-dimensional version of the divergence theorem. If we regard $\boldsymbol{B}$ as a fictitious magnetic field, then σ is the two-dimensional density of magnetic charge.

It turns out that in the strict adiabatic limit the vector field $\boldsymbol{B}$ is related to the theory of Berry phase [1, 2]. The formulation of this relation is as follows. Assume that the system is adiabatically cycled in the (X_1, X_2, X_3) space. In such a case, the Berry phase can be calculated as a line integral over a 'vector potential' (also called '1-form') $\boldsymbol{A}$. This can be converted by the Stokes theorem into a surface integral over a 'magnetic field' (also called '2-form') $\boldsymbol{B}$. The $\boldsymbol{B}$ field is defined as the 'rotor' of $\boldsymbol{A}$. It is a divergenceless field but it can have singularities which are known as 'Dirac monopoles'. These monopoles are located at $\vec{X}$ points where an occupied energy level has a degeneracy with a nearby level. Because of $\Phi \mapsto \Phi + (2\pi\hbar/e)$ gauge invariance, the Dirac monopoles form vertical chains as illustrated in figure 4(*b*). Hence, we have a distribution of what we call 'Dirac chains' [3, 4], which is characterized by a density $\sigma(X_1, X_2)$.

1.2. Background and objectives

Most of the literature about quantum pumping deals with the open geometry of figure 2(*b*). The most popular approach is the *S*-scattering formalism which leads to the Büttiker, Prêtre and Thomas (BPT) formula [5, 6] for the generalized conductance G. The BPT formula is

essentially a generalization of the Landauer formula. In previous publications [7, 4], we have demonstrated that the BPT formula can be regarded as a special limit of the Kubo formula. Our Kubo formula approach to pumping [3, 8] leads to 'level-by-level' understanding of the pumping process and allows us to incorporate easily non-adiabatic and environmental effects. In the strict adiabatic limit, it reduces in a transparent way to the theory of adiabatic transport [9, 10], also known as 'geometric magnetism' [2]. On the other hand, in the non-adiabatic(!) 'dc limit' of an open geometry it reduces to the S-matrix picture, hence resolving some puzzles that had emerged in older publications.

The question 'how much charge is pushed by translating a scatterer' has been addressed in [11] in the case of an open geometry using the BPT formula. We have addressed the corresponding problem of quantum stirring in closed geometry in a previous short publication [12], but the connection with the Dirac chains' picture has not been illuminated. Furthermore, in [12] only the quantum chaos limit was considered.

In the present paper, we put an emphasis on clarifying the route towards quantum-classical correspondence (QCC). We shall see that quantum-mechanical effects are pronounced in *simple* systems. As the system becomes more chaotic, QCC emerges. The Dirac chains' picture leads to new insights regarding the route towards QCC. These insights are easily missed if we stick to the formal Green function calculation of our earlier work [12]. From the above, it should be clear that the main objectives of the present study are the following:

- Derivation of a classical formula for Q (assuming a stochastic picture).
- Derivation of a quantum result for Q using the Dirac chains' picture.
- Exposing some counter-intuitive results for Q in the case of the simplest models.
- Illuminating the route towards QCC as we go from 'simple' to 'chaotic' systems.

We note that in [12] we have presented the classical formula for Q without the derivation.

1.3. Physical motivation and experimental feasibility

In the previous section, we have explained the theoretical motivations for dealing with the stirring problem. In the present section, we would like to further discuss the practicality of this line of study and the feasibility of actual experiments.

It is quite clear that the main focus of today's experiments is on *open* devices (with leads), whereas our interest is in *closed* devices. Our belief is that *'wireless'* mesoscopic or molecular size devices are going to be important building blocks of future 'quantum electronics'. This is of course a vision that people may doubt. However, on the scientific side our task is to analyse its feasibility.

It is possible to fabricate closed mesoscopic rings and to measure the persistent or the induced currents. Experiments with closed devices have been performed already 10 years ago. As an example, we mention [13] where a large array of rings has been fabricated. The current measurement has been achieved by coupling the rings to a highly sensitive electromagnetic superconducting micro-resonator.

The conceptually simplest way to drive a current is by inducing an electromotive force (EMF). In the setup of [13], the EMF has been induced by a 'wire' that spirals on top of the array. In our view, an attractive alternative option would be to induce currents by changing gate voltages so as to induce stirring. The advantage of such a possibility for the purpose of integrating wireless devices in future quantum electronics is quite obvious: it is much easier to control gate voltages than fluxes of magnetic field.

As far as *electronic devices* are concerned, there is no question about the feasibility of realizing quantum stirring by manipulating gate voltages and measuring the electrical currents.

But we would like to argue that such a possibility is also open in the case of *neutral atoms*. It is well known that 'billiards' that confine cold atoms can be realized and manipulated [14, 15]. Furthermore, there is no question regarding the possibility of creating a 'moving' optical barrier so as to create a stirring effect. There are a variety of techniques to measure the induced neutral currents. For example, one can exploit the Doppler effect at the perpendicular direction, which is known as the rotational frequency shift [16].

There is one more issue which might be of relevance in the case of an actual experiment. The Kubo formalism assumes that the system settles into a steady state, whereas the preparation in the case of an actual experiment is not very well controlled. We would like to argue that the results of the linear response analysis are quite robust. This issue is discussed in section 4 of [17]: what we get for Q in the Kubo analysis is not merely a formal result, but rather a prediction that has an actual physical significance.

1.4. Outline

In the first part of this paper, we review the result for G in the case of an open system using the BPT formula. Then we present two equivalent derivations of the corresponding *classical* result in the case of a closed geometry. We use the term 'classical' in the Boltzmann sense. This means that interference within the ring is neglected, while the reflection by the scatterers ('cross section') is calculated quantum mechanically. The first derivation is based on a direct solution of a master equation, while the second is a straightforward application of the Kubo formula. The classical calculation implies an expression for the density $\sigma(X_1, X_2)$ of the monopoles. The BPT formula implies $\sigma(X_1, X_2)$ that can be regarded as a special case of this calculation.

In the second part of this paper, we turn to the quantum-mechanical analysis. As a preliminary stage, we discuss the general conditions for having a degeneracy point $\vec{X}$ in the case of a one-dimensional ring. Then we review how the pumped charge Q can be estimated by calculating a line integral that encircles 'Dirac chains'. Thus, we realize that we have to figure out what the distribution $\sigma(X_1, X_2)$ of these chains looks like. Specifically, we consider the model systems that are illustrated in figure 1 and shown schematically in figure 2. The simplest is a ring where both g_1 and g_0 are modelled as delta barriers. The result for Q is quite remote from the classical expectation. Consequently, we try to figure out what happens to $\sigma(X_1, X_2)$ as the system becomes more complex: first, we add a second fixed barrier, and finally, we consider what happens in the case of a 'chaotic' barrier which is modelled using the random matrix theory. We make it clear that the route to the classical limit is intimately related to so-called 'quantum chaos' considerations.

2. Pushing particles in an open geometry

Let us consider the model of figure 2(b), where we have a scatterer within a single mode wire which is connected to two reservoirs with the same chemical potential. In this section, we assume non-interacting spinless electrons and zero-temperature Fermi occupation. The scatterer is described by

$$V(r; X_1, X_2) = X_2 \delta(r - X_1). \tag{2}$$

Hence, for some fixed values of X_1 and X_2 its transmission is

$$g_0(X_2) = \left[1 + \left(\frac{m}{\hbar^2 k_F} X_2\right)^2\right]^{-1}, \tag{3}$$

where m is the mass of the particle and k_F is the Fermi momentum. From now on, we work with units such that $\hbar = 1$. The S-matrix of the scattering region can be written in the general form

$$S = e^{i\gamma} \begin{pmatrix} -i\sqrt{1-g}\,e^{i\alpha} & \sqrt{g}\,e^{-i\phi} \\ \sqrt{g}\,e^{i\phi} & -i\sqrt{1-g}\,e^{-i\alpha} \end{pmatrix}, \tag{4}$$

where γ is the total phase shift, α is the reflection phase shift and $\phi = e\Phi/\hbar$ represents the flux which we assume to be zero. In the setup of figure 2(b), the length of the right lead is $L_A - X_1$ and the length of the left lead is $L_B + X_1$. Hence,

$$g = g_0, \tag{5}$$

$$\gamma = k_F(L_A + L_B) - \arctan\left(\frac{m}{\hbar^2 k_F}X_2\right), \tag{6}$$

$$\alpha = k_F(L_A - L_B) - 2k_F X_1. \tag{7}$$

Now that we know the dependence of the S-matrix on the parameters (X_1, X_2), the calculation of G is quite straightforward. We use the BPT formula

$$G^j = \frac{e}{2\pi i}\text{trace}\left(P_{\text{lead}}\frac{\partial S}{\partial X_j}S^\dagger\right), \tag{8}$$

where P_{lead} projects on the channels of the lead where the current is measured. As indicated in figure 2(b), the current is measured via a section which is located on the right lead. Using the BPT formula, we get

$$G^1 = -(1 - g_0)\frac{e}{\pi}k_F, \tag{9}$$

$$G^2 = -g_0\frac{e}{4\pi\hbar v_F}, \tag{10}$$

where v_F is the Fermi velocity corresponding to k_F. The result for G^1 is our main interest. It has been discussed in [11], where the term 'snow plow' has been coined in order to describe its physical interpretation. Namely, for zero-temperature Fermi occupation the density of electrons in the wire is k_F/π. Therefore, the number of electrons that are pushed by the scatterer is $dN = (k_F/\pi) \times dX_1$. If the transmission of the scatterer is not zero, some of the electrons pass through it and consequently we have to multiply dN by the reflection probability $1 - g_0$.

3. Stirring of particles in a closed geometry

Let us consider the model of figure 2(a), where the system is closed. We assume that the transmission of the ring without the moving scatterer is g_1^{cl}, while the transmission of the scatterer itself is g_0. In the following two subsections, we shall present two optional derivations of the 'classical' result for G. We use the term 'classical' in the Boltzmann sense. Namely, we regard the scattering from either g_1^{cl} or g_0 as a stochastic process. Thus, interference within the arms of the ring is not taken into account. For the sake of comparison with the BPT-based result, we still assume zero-temperature Fermi occupation (while in later sections we shall allow any arbitrary occupation). Within this framework, we obtain

$$G^1 = -\left[\frac{(1 - g_0)g_1^{\text{cl}}}{g_0 + g_1^{\text{cl}} - 2g_0 g_1^{\text{cl}}}\right]\frac{e}{\pi}k_F, \tag{11}$$
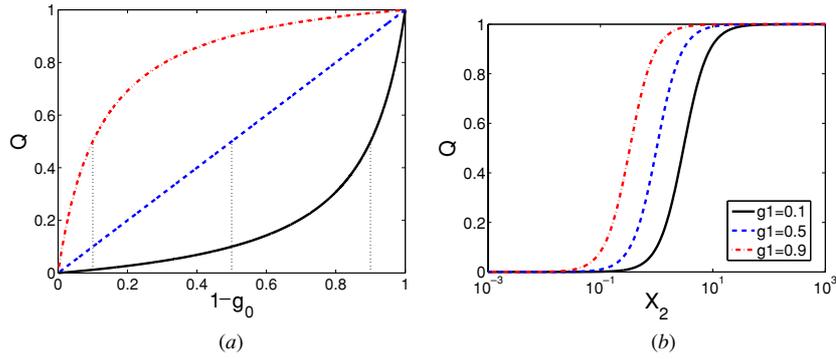
Figure 5. Plots of Q as a function of the 'size' of the scatterer. We use arbitrary units such that $Q = 1$ in the maximum. (*a*) Q is plotted against the reflection coefficient $(1 - g_0)$ for $g_1^{cl} = 0.1$, for $g_1^{cl} = 0.5$ and for $g_1^{cl} = 0.9$. The dotted lines highlight that Q for $g_0 = g_1^{cl}$ is half of its maximum value. Note that the BPT-based result corresponds to $g_1^{cl} = 0.5$. (*b*) Here Q is plotted against X_2 assuming that the scatterer is a delta function and setting $m/(\hbar^2 k_F) = 1$.

$$G^2 = -\left[\frac{(1 - g_1^{cl})g_0}{g_0 + g_1^{cl} - 2g_0 g_1^{cl}}\right]\frac{e}{4\pi\hbar v_F}. \tag{12}$$

We note that the amount of charge which is pushed by translating a scatterer by a distance ΔX_1 can also be written as [12]

$$Q = -G^1 \Delta X_1 = \left[\frac{1 - g_0}{g_0}\right]\left[\frac{g_T}{1 - g_T}\right]\frac{e}{\pi}k_F \times \Delta X_1, \tag{13}$$

where g_T is the overall transmission of the ring (including the moving scatterer) if it were opened:

$$\left[\frac{1 - g_T}{g_T}\right] = \left[\frac{1 - g_0}{g_0}\right] + \left[\frac{1 - g_1^{cl}}{g_1^{cl}}\right]. \tag{14}$$

As expected, the charge Q which is transported as a result of an X_1 displacement depends in a monotonic way on the reflection coefficient $1 - g_0$. It monotonically increases from zero and attains half of its maximal value for $g_0 = g_1^{cl}$. A plot of Q versus the 'size' of the scatterer is presented in figure 5 for three representative values of g_1^{cl}. We also plot Q against X_2, assuming that the scatterer is modelled as a delta function.

It is important to realize that the result for an *open geometry* is formally a special case corresponding to $g_1^{cl} = 1/2$. This value of g_1^{cl} means that memory is completely lost once a particle is scattered by the 'surroundings'. Namely, if $g_1^{cl} = 1/2$ then after a collision a particle has equal probability to go in either direction, and any information about its initial direction is lost. This observation generalizes our discussion in [18] regarding the relation between the Kubo and the Landauer conductance.

The classical expression for G implies the following result for the density $\sigma(X_1, X_2)$, which is illustrated in figure 6:

$$\sigma(X_1, X_2) = \frac{dB_2}{dX_2} = -\frac{em}{\pi\hbar^2}\frac{2(1 - g_1^{cl})g_1^{cl}}{\left[1 + \left(\left(\frac{m}{\hbar^2 k_F}X_2\right)^2 - 1\right)g_1^{cl}\right]^2}\left(\frac{m}{\hbar^2 k_F}X_2\right). \tag{15}$$
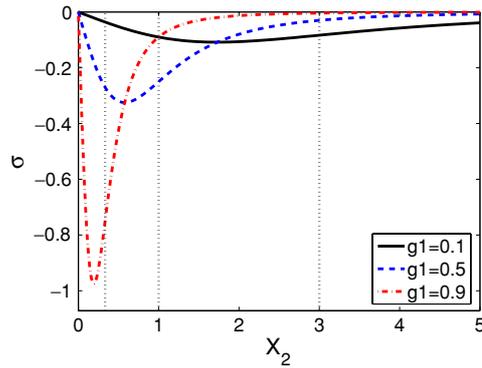
Figure 6. The classically deduced density σ as a function of X_2 for $g_1^{\text{cl}} = 0.1$, for $g_1^{\text{cl}} = 0.5$ and for $g_1^{\text{cl}} = 0.9$. We use arbitrary units for σ and set $m/(\hbar^2 k_F) = 1$. The dotted vertical lines correspond to the median X_2 values which are determined by the equation $g_0(X_2) = g_1^{\text{cl}}$.

In the following sections, we give two optional derivations of the classical result. The first derivation is based on a physically appealing master equation approach, in the spirit of the Boltzmann equation. The second derivation is a straightforward application of the Kubo formula. The calculation is done for G^1 and can easily be modified in order to get G^2. The advantage of the Kubo formula approach is that it can be generalized to the quantum-mechanical case, and it allows the incorporation of non-adiabatic and environmental effects.

4. Classical derivation using a master equation

We consider a ring with two scatterers: a moving scatterer g_0 whose velocity is $\dot{X}$ and a fixed scatterer g_1. A collision of a particle with the moving scatterer implies that its velocity is changed $v \mapsto v \pm 2\dot{X}$, where the sign depends on whether the collision is from the right or from the left. The associated change in the kinetic energy is $E \mapsto E \pm 2mv\dot{X} + \mathcal{O}(\dot{X}^2)$, respectively. There are two regions ($x < 0$ and $x > 0$) on the two sides of the g_0 scatterer. Accordingly, we have four distribution functions that satisfy the following balance equations:

$$\frac{\partial \rho_+^{\rightarrow}}{\partial t} = -\left[\rho_+^{\rightarrow} v\right] + g_0\left[\rho_-^{\rightarrow} v\right] + (1 - g_0)\left[\rho_+^{\leftarrow} v\right]_{E - 2mv\dot{X}}, \tag{16}$$

$$\frac{\partial \rho_+^{\leftarrow}}{\partial t} = -\left[\rho_+^{\leftarrow} v\right] + g_1\left[\rho_-^{\leftarrow} v\right] + (1 - g_1)\left[\rho_+^{\rightarrow} v\right], \tag{17}$$

$$\frac{\partial \rho_-^{\rightarrow}}{\partial t} = -\left[\rho_-^{\rightarrow} v\right] + g_0\left[\rho_+^{\rightarrow} v\right] + (1 - g_0)\left[\rho_-^{\leftarrow} v\right], \tag{18}$$

$$\frac{\partial \rho_-^{\leftarrow}}{\partial t} = -\left[\rho_-^{\leftarrow} v\right] + g_1\left[\rho_+^{\leftarrow} v\right] + (1 - g_1)\left[\rho_-^{\rightarrow} v\right]_{E + 2mv\dot{X}}. \tag{19}$$

The zero-order solution in $\dot{X}$ is to have all the four distribution functions equal to some arbitrary function $f(E)$. In the presence of driving, assuming that the system has reached a steady state, we still have to satisfy the two $\dot{X}$-free equations, leading to

$$\rho_+^{\leftarrow} = g_1\rho_-^{\leftarrow} + (1 - g_1)\rho_+^{\rightarrow}, \tag{20}$$

$$\rho_-^{\rightarrow} = g_1\rho_+^{\rightarrow} + (1 - g_1)\rho_-^{\leftarrow}. \tag{21}$$

Substitution into the other two equations leads after linearization to

$$\rho_+^{\rightarrow}(E) - \rho_-^{\leftarrow}(E) = -2mv\dot{X}\left(\frac{1-g_0}{g_0+g_1-2g_0g_1}\right)\frac{\partial f(E)}{\partial E}, \tag{22}$$

and for the current we get

$$I = \int_0^\infty \frac{\mathrm{d}p}{2\pi}\left(\rho_\pm^{\rightarrow} - \rho_\pm^{\leftarrow}\right)ev = \int_0^\infty \frac{\mathrm{d}p}{2\pi}g_1\left(\rho_+^{\rightarrow} - \rho_-^{\leftarrow}\right)ev \tag{23}$$

$$= -\dot{X}\int_0^\infty\left[\frac{e}{\pi}\left(\frac{(1-g_0)g_1}{g_0+g_1-2g_0g_1}\right)mv\right]\frac{\partial f(E)}{\partial E}\,\mathrm{d}E. \tag{24}$$

With the assumption of zero-temperature Fermi occupation, this gives the cited result for G^1.

5. Classical derivation using the Kubo formula

The generalized fluctuation–dissipation version of the Kubo formula (see [4] and further references therein) relates the generalized conductance to the cross-correlation function of the current $\mathcal{I}$ and the generalized force $\mathcal{F} = -\partial\mathcal{H}/\partial X$. If X is the displacement X_1 of the scatterer, then

$$\mathcal{F} = -\frac{\partial\mathcal{H}}{\partial X_1} = X_2\delta'(x - X_1). \tag{25}$$

For the sake of comparison with previous results, we assume zero-temperature Fermi occupation. Then the Kubo formula takes the form

$$G = g(E_\mathrm{F})\int_0^\infty \langle\mathcal{I}(\tau)\mathcal{F}(0)\rangle\,\mathrm{d}\tau = \frac{L}{\pi\hbar v_\mathrm{F}}\langle\mathcal{Q}\mathcal{F}\rangle, \tag{26}$$

where $g(E) = L/(\pi\hbar v_\mathrm{F})$ is the density of states. This density of states is proportional to the total 'volume' of the network which is L. In the second expression, we got rid of the time by introducing the notation

$$\mathcal{Q} = \int_0^\infty \mathcal{I}(\tau)\,\mathrm{d}\tau. \tag{27}$$

It should be clear that both the generalized force $\mathcal{F}$ and the transported charge $\mathcal{Q}$ are functions in phase space and that $\langle\cdots\rangle$ stands for phase space average over position and velocity. For $\mathcal{F}$, we already have an explicit expression (equation (25)). Now we have to figure out what is $\mathcal{Q}$.

On the ring there are two scatterers and one point $x = x_0$ where the current is measured. Hence, the ring is divided into three segments. In addition, there are two possible directions of motion (clockwise, anticlockwise). Hence, the phase space is divided into six regions. It is obvious that the outcome from equation (27) depends merely on which region the classical trajectory had started its journey. In fact, we need to consider only the four regions where the particle starts in the vicinity of the moving scatterer, else $\mathcal{F}$ vanishes. So we have the '+' region between the moving scatterer and x_0, and the '−' region on the other side between the two scatterers. Accordingly, the four possible outcomes from equation (27) are

$$Q_+^{\rightarrow} = e\left[\frac{1}{2(1-g_\mathrm{T})}\right], \tag{28}$$

$$Q_+^{\leftarrow} = -e\left[\frac{1}{2(1-g_\mathrm{T})} - 1\right], \tag{29}$$

$$Q_-^\rightarrow = \left[\frac{g_0}{1-(1-g_1)(1-g_0)} - \frac{g_1(1-g_0)}{1-(1-g_1)(1-g_0)} \right] Q_+^\rightarrow = \frac{g_0 - g_1 + g_0 g_1}{g_0 + g_1 - g_0 g_1} Q_+^\rightarrow, \quad (30)$$

$$Q_-^\leftarrow = -\frac{g_1 - g_0 + g_0 g_1}{g_0 + g_1 - g_0 g_1} Q_+^\rightarrow. \tag{31}$$

The derivation of the above expressions is as follows. It is simplest if the particle starts in the '+' region, because then we can regard the two scatterers as one effective scatterer g_T. Assume that at time $t = 0$ the particle approaches $x = x_0$ from the left. The charge that goes through the section after a round trip is suppressed by a factor $(2g_T - 1)$ due to the scattering (we sum the clockwise and anticlockwise contributions). Thus, we find that the total charge that goes through the section due to multiple reflections is a geometric sum that leads to equation (28). If we start in the '+' region in the opposite direction, then we have the same sequence but with the opposite sign and without the first term. Hence, we get equation (29). Next assume that at $t = 0$ the particle starts in the '−' region and approaches g_0 from the left. Then we can have at a later time a positive pulse of current. The probability for that is the geometric summation over $g_0((1 - g_0)(1 - g_1))^{\text{integer}}$. Otherwise, we get a negative pulse of current, with a complementary probability that can be regarded as a geometric summation over $g_1((1 - g_0)(1 - g_1))^{\text{integer}}(1 - g_0)$. Thus, the total current through the section, taking into account all subsequent multiple reflections (rounds), is given by equation (30). A similar calculation leads to equation (31).

Since there are only four possible values for $\mathcal{Q}$, the calculation of the phase space average becomes trivial:

$$\langle \mathcal{Q} \mathcal{F} \rangle = \frac{1}{2L} \left[\int_+ \mathcal{F} \, dr \right] Q_+^\rightarrow + \frac{1}{2L} \left[\int_+ \mathcal{F} \, dr \right] Q_+^\leftarrow + \frac{1}{2L} \left[\int_- \mathcal{F} \, dr \right] Q_-^\rightarrow + \frac{1}{2L} \left[\int_- \mathcal{F} \, dr \right] Q_-^\leftarrow.$$

The integral over $\mathcal{F}$ is taken either within the '+' region or within the '−' region. It is trivially related to the momentum impact and yields the result

$$\int_\pm \mathcal{F} \, dr = \mp m v_F^2. \tag{32}$$

Putting everything together, we get the desired result for G^1. With some minor modifications, we can calculate G^2 using the same procedure.

6. The quantum-mechanical picture

The Kubo formula also holds in the quantum-mechanical case. But now $\mathcal{I}$ and $\mathcal{F}$ are operators, so it is more convenient to express the Kubo formula using their matrix elements. After some algebra, one obtains the result

$$G = \sum_{m(\neq n)} \frac{2\hbar \, \text{Im}[\mathcal{I}_{nm}] \mathcal{F}_{mn}}{(E_m - E_n)^2 + (\Gamma/2)^2}. \tag{33}$$

For more details see [4] and further references therein. In the above formula, it is assumed that only one energy level (n) is occupied. If we have zero-temperature Fermi occupation, then we have to sum over all the occupied levels. The Kubo formula incorporates a parameter Γ that reflects either the non-adiabaticity of the driving or the environmentally induced 'memory loss' due to decoherence. For a strictly isolated system in the strict adiabatic limit, we have $\Gamma = 0$. Then we identify G as an element of Berry's field B, as explained in the introduction. The effect of Γ on B will be discussed below.

We would like to see how the classical result can emerge in some limit from the above quantum expression. It turns out that this does not require a detailed calculation. We can use some topological properties of B in order to figure out the answer! The main observations that we further explain below are as follows:

(1) B is divergenceless with the exception of Dirac monopoles.
(2) The monopoles are arranged in $\vec{X}$ space as vertical chains.
(3) The far field of B is like a two-dimensional electrostatic problem.
(4) Only non-compensated chains give net contribution.

As long as the occupied level n does not have a degeneracy with a nearby level, B is finite and divergenceless. Only at degeneracies can it become singular. It can be argued that these singularities must have their charge quantized in units of $\hbar/2$ else the Berry phase would be ill defined. We have defined $X_3 = \Phi$ as the Aharonov–Bohm flux through the ring. This means that if we change X_3 by $2\pi\hbar/e$ then by gauge invariance we have another degeneracy. This means that the Dirac monopoles are arranged as vertical chains and that the average charge per unit length is $e/(4\pi)$. Thus, the far field of a Dirac chain is as in a two-dimensional electrostatic problem. If we calculate the line integral of equation (1), then we get, within the framework of the far field approximation, $Q = 1$. Thus, we conclude that if we have several Dirac chains of the same 'sign', then Q simply counts how many are encircled.

We have to note that if we have Fermi occupation then the *net* contribution comes only from degeneracies of the last occupied level with the first unoccupied level. This is what we meant above (item (4)) by 'non-compensated'. In order to avoid misunderstanding of the 'compensation' issue, let us discuss in some more detail what happens if two neighbouring levels n and m are occupied. With the level n we associate a field $B^{(n)}$, while with m we associate a field $B^{(m)}$. In general, $B^{(m)} \neq -B^{(n)}$. If we are near a degeneracy, then we may say that $B^{(n)}$ emerges from a Dirac chain which is associated with level n, while $B^{(m)}$ emerges from a Dirac chain which is associated with level m. By inspection of equation (33), taking into account that $\mathrm{Im}[\mathcal{I}_{nm}] = -\mathrm{Im}[\mathcal{I}_{mn}]$, we realize that the two Dirac chains have opposite charge. Their corresponding fields do not cancel each other, but the total field is no longer singular, implying that the *net* charge is zero.

In the quantum stirring problem, we shall see that the X_1 distance between non-compensated chains is simply half of the De-Broglie wavelength $\lambda_E = 2\pi/k_E$. From this it follows that the amount of charge which is pushed by a very 'large' scatterer is

$$Q \approx e \frac{\Delta X_1}{\lambda_E/2} = e \frac{k_E}{\pi} \times \Delta X_1. \tag{34}$$

What happens if the cycle is not in the 'far field' but rather passes through the distribution of the monopoles? To be more specific, let us consider what happens to Q if we displace the scatterer by a distance ΔX_1. What is the dependence on X_2? Do we get the classical result as in figure 5? Obviously, in order to get the classical result the distribution $\sigma(X_1, X_2)$ should be in accordance with equation (15). Strictly speaking, this is *not* the case because we have a discrete set of monopoles rather than a smooth distribution of 'magnetic charge'. Still we can hope that $\sigma(X_1, X_2)$ would be classical-like upon course graining. We discuss further this issue in the next paragraphs.

If we make a pumping cycle in the vicinity of a monopole, then it is obvious that the result would be very different from the classical prediction. What we expect to get in the quantum-mechanical case is illustrated in the upper panel of figure 7. For a cycle that goes very close to a monopole, the charge can be huge. In reality, it is very difficult to satisfy the adiabatic condition near a degeneracy, or else there are always environmental effects. Either way, once we have a finite Γ, the result that we get for Q is smoothed.
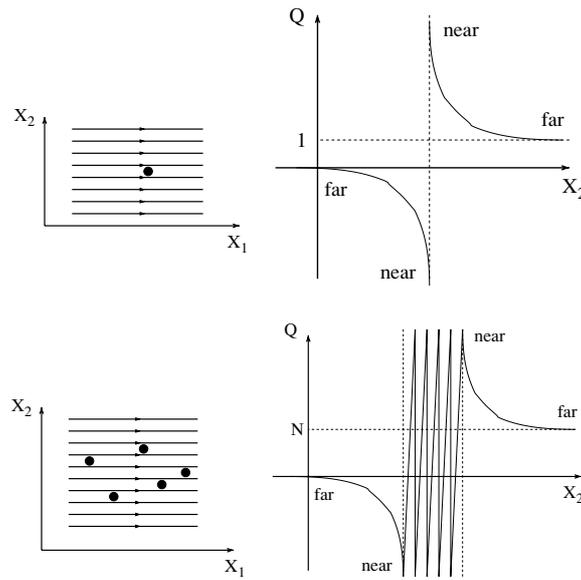
Figure 7. Several pumping cycles are indicated in the left panel. It is implicit that each segment is closed as in figure 3. The black points represent degeneracies. For each pumping cycle, one can calculated Q. The qualitative expectation for the outcome is illustrated in the right panel. In the upper illustration we assume that the pumping cycle encircles only one degeneracy, while in the lower illustration we assume that it encircles N degeneracies. In a later section, we display numerical results that support the illustrated expectations.

If the pumping cycle passes through a distribution of many monopoles, then what we expect to get (as we deform or shift the cycle) are huge fluctuations as illustrated in the lower panel of figure 7. Again, the effect of either non-adiabaticity or environmental effects is to smooth away these fluctuations. The interested reader can find some further discussion of this point including a numerical example in [12].

Coming back to the quantum-classical correspondence (QCC) issue, we realize that at best QCC can be satisfied in a statistical sense. So we ask whether the coarse-grained $\sigma(X_1, X_2)$ agrees with the classical expectation equation (15). The answer which we give in the following sections is that QCC is not realized in the case of simple non-chaotic models. In the 'simple' cases, we get a non-classical $\sigma(X_1, X_2)$ and hence a different dependence of Q on X_2.

7. The degeneracies in X space

We can use the scattering approach in order to find the energy levels of a ring. In this approach, the ring is opened at some arbitrary point and the S-matrix of the open segment is specified. It is more convenient to use the row-swapped matrix, such that the transmission amplitudes are along the diagonal:

$$\tilde{\boldsymbol{S}}(E; X_1, X_2) = e^{i\gamma} \begin{pmatrix} \sqrt{g}\, e^{i\phi} & -i\sqrt{1-g}\, e^{-i\alpha} \\ -i\sqrt{1-g}\, e^{i\alpha} & \sqrt{g}\, e^{-i\phi} \end{pmatrix}. \tag{35}$$

The periodic boundary conditions imply the following secular equation:

$$\det(\tilde{\boldsymbol{S}}(E; X_1, X_2) - \boldsymbol{1}) = 0. \tag{36}$$

Using

$$\det(\tilde{S} - I) = \det(\tilde{S}) - \text{trace}(\tilde{S}) + 1, \tag{37}$$

$$\det(\tilde{S}) = (e^{i\gamma})^2, \tag{38}$$

$$\text{trace}(\tilde{S}) = 2\sqrt{g}\, e^{i\gamma} \cos\phi, \tag{39}$$

we get

$$\cos(\gamma(E)) = \sqrt{g(E)} \cos(\phi). \tag{40}$$

In order to find the eigenenergies, we plot both sides as a function of E. The left-hand side oscillates between -1 and $+1$, while the right-hand side may have a smaller amplitude. It is not difficult to realize that the only way to have two eigenenergies coincide is to get

$$\begin{Bmatrix} \phi = 0 \bmod(2\pi) \\ g = 1 \\ \gamma = n_{\text{even}}\pi \end{Bmatrix} \quad \text{or} \quad \begin{Bmatrix} \phi = \pi \bmod(2\pi) \\ g = 1 \\ \gamma = n_{\text{odd}}\pi \end{Bmatrix}, \tag{41}$$

where n is either an even or an odd integer that can be exploited (if we keep track over γ) as a level counter.

Both g and γ depend on $(E; X_1, X_2)$. Since we want g to be maximal, the condition for having a degeneracy involves four rather than three equations as we are going to see below. An immediate conclusion is that we have two types of Dirac chains: those that have monopoles in the plane of the pumping cycle ($X_3 = \Phi = 0$) and those that have monopoles off the plane of the pumping cycle.

In our model system, we have two scatterers. One is the moving scatterer and the other is the rest of the network. The two are connected by arms of length $L_A - X_1$ and $L_B + X_1$. The constants L_A and L_B can be absorbed into the definition of the surrounding network. Each scatterer is fully characterized by the set of parameters $\{g_i, \gamma_i, \alpha_i, \phi_i\}$. Note that we do not absorb X_1 into the definition of α_0. After some algebra, we find the following expressions for the transmission coefficient and for the total phase shift:

$$g = \frac{g_0 g_1}{2 - g_0 - g_1 + g_0 g_1 + 2\sqrt{(1 - g_0)(1 - g_1)} \cos(\gamma_0 + \gamma_1 + \alpha_0 + \alpha_1 - 2k_E X_1)}, \tag{42}$$

$$\gamma = \gamma_0 + \gamma_1, \tag{43}$$

where k_E is the wave number that corresponds to the energy E. Thus, the conditions for having a degeneracy take the form

$$\begin{cases} X_3 = \text{integer flux} \\ g_0(X_2) = g_1 \\ \alpha_0 + \alpha_1 - 2k_E X_1 = \pi \bmod(2\pi) \\ \gamma_0 + \gamma_1 = n_{\text{even}}\pi, \end{cases} \quad \begin{cases} X_3 = \text{half integer flux} \\ g_0(X_2) = g_1 \\ \alpha_0 + \alpha_1 - 2k_E X_1 = 0 \bmod(2\pi) \\ \gamma_0 + \gamma_1 = n_{\text{odd}}\pi. \end{cases} \tag{44}$$

We have highlighted the dependence on the parameters (X_1, X_2, X_3). There is of course also an implicit dependence of $\{g_i, \gamma_i, \alpha_i\}$ on the energy E. The conditions that are listed above are very intuitive: the system should have time reversal symmetry, the barriers should 'balance' each other, the phases which are associated with the reflections should lead to destructive interference and the total phase shift should respect the periodic boundary conditions.

From the third condition of equation (44), we see that in general the X_1 distance between degeneracies that belong to the same level is roughly half of the De-Broglie wavelength as
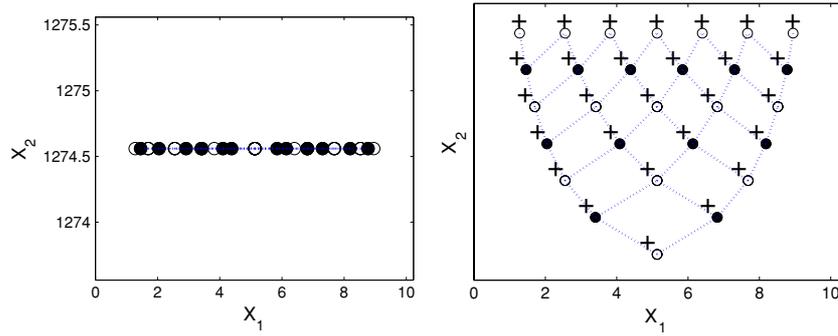
Figure 8. The degeneracies in the double delta model of figure 1. We set $L_A = 10.23$ and $L_B = 0$, so that X_1 measures the distance from the fixed scatterer. The 'size' of the fixed delta scatterer is $V = 1274.56$. We use units such that $m = \hbar = 1$. We assume that only the lower seven levels are occupied. The filled circles are degeneracies on the flux zero plane and the empty circles are degeneracies on the flux π plane. The left graph shows the actual arrangement in the (X_1, X_2) plane. Namely, all the degeneracies are on the line $X_2 = V$. In the right graph, the degeneracies were displaced for the sake of clarity. Only the seventh occupied level contributes non-compensated monopoles.

stated previously. The question that we would like to address is how these degeneracies are distributed with respect to X_2.

8. Quantum stirring in simple rings

We would like to find the distribution of degeneracies with respect to X_2 in the simplest model: a ring with two delta scatterers (see figure 1). The arms that connect the two scatterers are of length $L_A + X_1$ and $L_B - X_1$. For the S-matrix that represents the fixed scatterer (including the arms), we have

$$g_1(E) = \left[1 + \left(\frac{m}{\hbar^2 k_F} V \right)^2 \right]^{-1}, \tag{45}$$

$$\gamma_1(E) = k_E(L_A + L_B) - \arctan\left(\frac{m}{\hbar^2 k_F} X_2 \right), \tag{46}$$

$$\alpha_1(E) = k_E(L_A - L_B). \tag{47}$$

Since the dependence of g_0 and g_1 on the barrier 'size' has the same functional form, the third condition of equation (44) implies $X_2 = V$ irrespective of E. Thus, we get that all the degeneracies are concentrated at the same X_2. This is clearly very different from the classically expected distribution.

In figure 8, we display an example. The degeneracies that are associated with the first seven levels are indicated. Filled circles stand for $\phi = 0$ degeneracies, while hollow circles stand for $\phi = \pi$ degeneracies. Only the last (seventh) level contributes non-compensated monopoles. The X_1 distance between the non-compensated monopoles is roughly half of the De-Broglie wavelength.

In figure 9, we show what happens to the degeneracies if we add a second fixed scatterer. We have chosen an additional scatterer that can be treated as a perturbation. The calculation was done using perturbation theory. We shall not present the details of this lengthy calculation
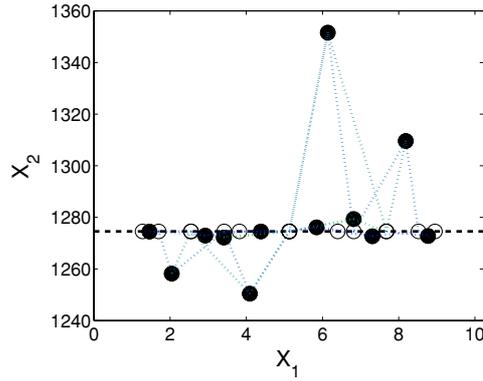
Figure 9. The degeneracies in the triple delta model of figure 1. Namely, to the model of figure 8 we have added a delta barrier of 'size' $V_P = 10^{-5}$, located at $x = 7.61$. This additional delta barrier can be treated as a small perturbation. As a result of this perturbation, the degeneracies shift and spread out in the X_2 direction. Degeneracies that belong to the same level are connected by a line. As in the previous figure, only the seventh occupied level contributes non-compensated monopoles.
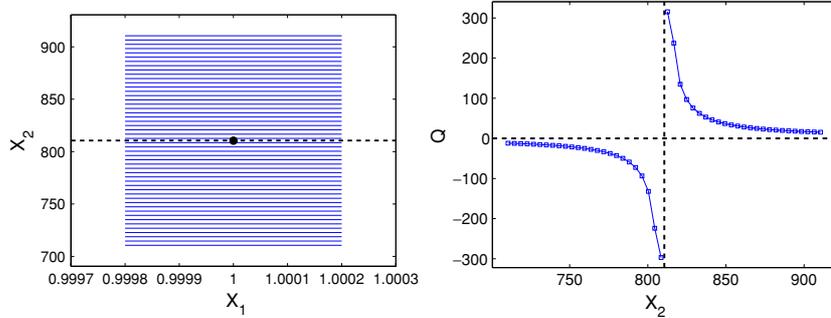

Figure 10. Several pumping routes are displayed in the left panel. For each of them, Q has been calculated numerically. The results are displayed in the right panel. Note the agreement with the qualitative expectation that has been expressed in figure 7. The calculation is done for the double delta model of figure 1 with $L_A = 1000.23$ and $L_B = 0$. The 'size' of the fixed barrier is $V = 810.56$. The energy levels involved are $n = 998$ and $m = 999$. We use units such that $m = \hbar = 1$.

here. For larger perturbations (not presented), we had to solve the secular equation numerically. This was done using an efficient algorithm[1]. In any case, the purpose of figure 9 is merely to demonstrate that once the symmetry of the system is broken the degeneracies spread out in the X_2 direction.

The distribution $\sigma(X_1, X_2)$ in the case of a ring with a single fixed scatterer is very different from the classical prediction. Consequently, also Q comes out very different from equation (15) (and see also figure 6). The reader might be curious to know how Q depends on the 'size' (X_2) of the scatterer in the case of Fermi occupation. So we have calculated G numerically using equation (33) and integrated over it to get Q. The numerical results are displayed in figure 10. Further analysis of the crossover from 'near-field' to 'far-field' cycles will be published in a separate work [17].

---

[1] We thank H Schanz for suggesting the numerical algorithm.
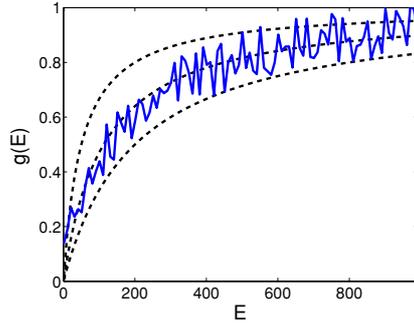
Figure 11. A hypothetical illustration of $g_1(E)$ in the case of a complex 'chaotic' barrier. Such a barrier can be modelled as a network (figure 1(*a*)), or it can be characterized using the random matrix theory. The smooth curves are the transmission $g_0(E; X_2)$ of the delta scatterer for three different values of X_2.

9. Quantum stirring in chaotic rings

We would like to find the distribution of degeneracies with respect to X_2 in the case of a chaotic network (see an example in figure 1). Let us try to extend the approach that has been used in the previous section. A hypothetical illustration of $g_1(E)$ in the chaotic case is displayed in figure 11. The universal conductance fluctuations of g_1 are characterized by a one-parameter probability distribution $P(g_1; \bar{g}_1)$ which we discuss below. This probability distribution depends on one parameter, which we choose to be the average transmission $\bar{g}_1$.

In order to get a degeneracy, a necessary but insufficient condition is that the transmission of the two barriers is equal ($g_0(E; X_2) = g_1(E)$). The solution of this equation can be determined graphically via figure 11. In fact, in most practical applications we can assume that our interest is restricted to some small energy window such that the smooth E dependence of g_0 can be neglected. So the equation is in fact $g_0(X_2) = g_1(E)$. For a given E, we can find an $X_2^{(E)}$ such that this equation is satisfied. By playing with X_1, we can satisfy the α-related phase condition for having a degeneracy. But we still have to also satisfy the γ-related phase condition, which leads to the quantization of the energy E. Hence, the erratic $X_2^{(E)}$ is sampled. Still it is reasonable to assume that the distribution of the so-obtained X_2 values is not affected by this random-like sampling. We therefore conclude the following relation:

$$\text{Prob}\left[X_2 < X_2^{(E)} < X_2 + dX_2\right] = \text{Prob}[g_0(X_2) < g_1 < g_0(X_2 + dX_2)]. \quad (48)$$

This implies a simple relation between $\sigma(X_1, X_2)$ and the probability function $P(g_1; \bar{g}_1)$

$$\sigma(X_1, X_2) = \text{const} \times \frac{dg_0(X_2)}{dX_2} P(g_0(X_2)). \quad (49)$$

Thus, the problem of finding $\sigma(X_1, X_2)$ has reduced to the problem of finding $P(g_1; \bar{g}_1)$.

We can now proceed in three directions: (a) to determine $P(\cdot)$ from simple heuristic quantum chaos considerations; (b) to determine $P(\cdot)$ from formal random matrix theory considerations; (c) to use reverse engineering in order to determine what is $P(\cdot)$ that would give the classical result. It should be clear that universality can be expected only if $\bar{g}_1 \ll 1$. In figure 12, we make a comparison between the outcomes of these three procedures for $\bar{g}_1 = 0.001$. In the following paragraph, we give the details of the calculation.

The heuristic approach is based on the idea that the transmission via a chaotic network depends on the amplitudes of the wavefunctions at the entrance and exit points. One
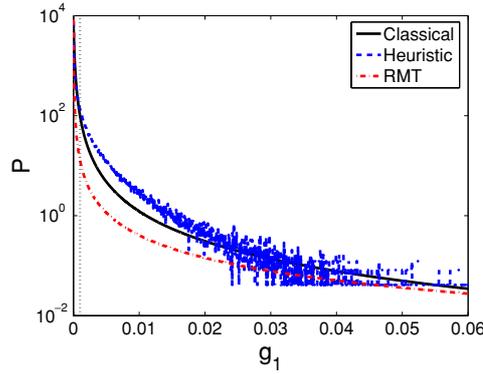
Figure 12. A plot of the distribution $P(g_1; \bar{g}_1)$ according to several different expressions. In this calculation, we assume that the average transmission is $\bar{g}_1 = 0.001$, which is represented in the figure by a vertical dashed line. The 'heuristic' result is based on sampling of the random variable $g_1 = \bar{g}_1 \eta_1 \eta_2$, where η is Porter–Thomas distributed. The 'RMT' result is based on equation (50). The 'classical' result is based on equation (51).

might expect $g_1 = \bar{g}_1 \eta_1 \eta_2$, where η has the Porter–Thomas distribution [19] $P_{\text{GOE}}(\eta) = (1/\sqrt{2\pi\eta})\, e^{-\eta/2}$. This leads to the 'heuristic' result in figure 12. In fact, this result should not be taken too seriously. The formal RMT calculation [20] of the probability distribution $P(g_1; \bar{g}_1)$ leads to the following expressions:

$$P_{\text{RMT}}(g_1; \bar{g}_1) = \begin{cases} (2/\pi^2 \bar{g}_1) g_1^{-1/2} & \text{for } g_1 \ll (\bar{g}_1)^2 \ll 1, \\ (4\bar{g}_1/\pi^2) g_1^{-3/2} & \text{for } (\bar{g}_1)^2 \ll g_1 \ll 1. \end{cases} \tag{50}$$

The small g_1 approximation is universal: it merely assumes that the system has time reversal symmetry. It has been confirmed [21] that this universal behaviour also holds for network systems. But for larger values of g_1 there are deviations that has to do with semiclassical considerations. It is therefore in the latter region where one might expect quantum-classical correspondence.

The probability distribution $P(g_1; \bar{g}_1)$ that would reproduce the classical result (equation (15)) via equation (49) is

$$P_{\text{CL}}(g_1; \bar{g}_1) = \frac{(1 - g_1^{\text{cl}}) g_1^{\text{cl}}}{(g_1 + g_1^{\text{cl}} - 2g_1 g_1^{\text{cl}})^2}, \tag{51}$$

with $g_1^{\text{cl}} \approx 0.12 \bar{g}_1$. In order to compare with the RMT result, we note that

$$P_{\text{CL}}(g_1; \bar{g}_1) \approx \begin{cases} (1/g_1^{\text{cl}})(1 - 2g_1/g_1^{\text{cl}}) & \text{for } g_1 \ll g_1^{\text{cl}} \ll 1, \\ g_1^{\text{cl}} \, g_1^{-2} & \text{for } g_1^{\text{cl}} \ll g_1 \ll 1. \end{cases} \tag{52}$$

We see that in the large g_1 region, where one might expect quantum-classical correspondence, there is no agreement between $P_{\text{CL}}(\cdot)$ and $P_{\text{RMT}}(\cdot)$. We suspect that $P_{\text{RMT}}(\cdot)$ cannot be trusted there. Otherwise we have to conclude that equation (49) fails to take into account strong correlations in the arrangement of Dirac monopoles. Either way, it seems that RMT alone is not enough in order to reproduce the classical result.

10. The emergence of the classical limit

With simple minded RMT reasoning, we have failed to get a quantitative correspondence with the classical result. We therefore look for a different way to get an estimate for either B_2

or $\sigma(X_1, X_2)$ in the case of a chaotic network. One obvious way is to use the result of [22] regarding the distribution of degeneracies (diabolic points). The perturbation term which is associated with X_2 is

$$\mathcal{W} = \frac{\partial \mathcal{H}}{\partial X_2} = \delta(x - X_1), \tag{53}$$

and the density of the degeneracies should be [22]

$$\sigma(X_1, X_2) = \frac{\pi}{3} g(E)^2 \text{RMS}[\mathcal{F}_{nm}] \text{RMS}[\mathcal{W}_{nm}] \propto \text{RMS}[\mathcal{W}_{nn}], \tag{54}$$

where $g(E)$ is the density of states. In the first equality, it is implicit that the root mean square (RMS) of *near-diagonal* matrix elements should be estimated. In fact, only $\text{RMS}[\mathcal{W}_{nm}]$ is required in order to find the X_2 dependence. For a quantum chaos system with time reversal symmetry, the variance of the near-diagonal elements equals half of the variance of the diagonal elements [23], leading to the second expression.

There is a well-known semiclassical recipe [24, 25] for calculating the variance of the near-diagonal matrix elements $\mathcal{W}_{nm}$. One should find the classical correlation function $C(\tau) = \langle \mathcal{W}(t)\mathcal{W}(0)\rangle - \langle \mathcal{W}\rangle^2$, and then integrate over τ. If $\mathcal{W}$ were the current operator, then $\langle \mathcal{W}\rangle$ would be equal to zero, and we could proceed as in section 5. But in the case of equation (53) there is a problem: the sign of $\mathcal{W}(t)$ does not fluctuate, and it is essential to take into account the distribution of the delay times inside the network. Therefore, there is no obvious relation to the transmissions g_0 and g_1.

An optional possibility is to try to evaluate $\text{RMS}[\mathcal{W}_{nn}]$, where $\mathcal{W}_{nn} = |\psi_{\text{barrier}}|^2$ is the 'intensity' of the wavefunction at the location of the scatterer. Obviously, the result depends on both g_0 and g_1, and requires considerations which are at least as difficult as estimating universal conductance fluctuations. So it seems that we would run into the same problems as in the previous section.

Still there is the option to calculate $G^1 = B_2$ from the Green function of the system. This has been done in [12]: writing the Green function as a sum over trajectories, we have expressed G^1 as a double sum over paths. If this double sum is averaged over the energy, one obtains the diagonal approximation, leading to the classical result. At the first glance, the energy averaging is not quite legitimate, because the energy is quantized. But one can justify this procedure in the case of a 'quantum chaos system'. We have further supported this claim by the numerical analysis of the chaotic network of figure 1 [12]. We therefore conclude that for a chaotic network the distribution of degeneracies should be in accordance with equation (15).

11. Conclusions

As we translate a scatterer of 'size' X_2 by a distance ΔX_1 along a single mode wire, the amount of charge which is pushed is

$$Q = r(X_2) \times \frac{e}{\pi} k_F \times \Delta X_1, \tag{55}$$

where k_F is the Fermi momentum. If the scatterer is very 'large' ($X_2 \to \infty$), then we expect to have $r(X_2) = 1$. This expectation is based on the 'snow plow' picture that has been explained in the conclusion of section 2. This result is also confirmed by the formal BPT-based calculation in the case of an *open* geometry. It can also be formally derived for a *closed* geometry using the 'Dirac chains' picture'. In the latter case, the key observation is that the X_1 distance between contributing degeneracies is roughly half of the De-Broglie wavelength. See equation (34).

Next we ask what happens to $r(X_2)$ as X_2 becomes smaller. In the case of an *open* geometry, the intuitive naive guess, which is based on the 'snow plow' picture, turns out to be correct. Namely, $r(X_2) = 1 - g_0$ is simply the reflection coefficient: some of particles are not 'pushed' by the scatterer because of its partial transparency. In the case of a *closed* geometry, we have shown that the *classical* result for $r(X_2)$ is modified: now it also depends on the overall transmission of the device. See equation (13).

It is important to realize that the *classical* result for $r(X_2)$ is in complete agreement with the common sense expectation. Namely, we have $0 < r(X_2) < 1$, and the dependence on the 'size' of the scatterer is monotonic. But once we go to the quantum-mechanical analysis, we have a surprise. The results that we get are counter-intuitive. They are most puzzling (figure 10) in the case of the simplest model, in which the ring contains only one fixed delta barrier (V). As we decrease X_2, the transported charge Q becomes larger(!). Moreover, once X_2 becomes smaller than V, the coefficient $r(X_2)$ changes sign. This means that as we push the particles 'forward' the current is induced 'backwards'.

The reason for the failure of our intuition is our tendency to regard 'adiabatic transport' as a zero-order adiabatic approximation, while in fact it is based on a first-order analysis (for a detailed discussion see section 4 of [17]). As a parameter in the system is changed, the induced current can be in either direction.

In order to understand the route towards quantum-classical correspondence, it is essential to figure out how the degeneracies spread out in $\vec{X}$ space. As the system becomes more complex, we get for $r(X_2)$ a result that resembles the classically implied one. The resemblance is at best only on a coarse-grained scale: the quantum result has strong fluctuations. These are related to universal conductance fluctuations.

We have made an attempt to deduce from RMT considerations the 'chaotic' distribution of the degeneracies, and hence the dependence of $r(X_2)$ on X_2. The quantitative results do not agree. We therefore suspect that RMT considerations alone are not enough in order to establish quantum-classical correspondence. Rather, we had used [12] semiclassical tools in order to establish this correspondence.

References

[1] Berry M V 1984 *Proc. R. Soc.* A **392** 45
[2] Berry M V and Robbins J M 1993 *Proc. R. Soc.* A **442** 659
[3] Cohen D 2003 *Phys. Rev.* B **68** 155303
[4] For a mini-review and further references see Cohen D 2005 *Physica* E **29** 308
[5] Büttiker M *et al* 1994 *Z. Phys. B: Condens. Matter* **94** 133
[6] Brouwer P W 1998 *Phys. Rev.* B **58** R10135
[7] Cohen D 2003 *Phys. Rev.* B **68** 201303
[8] Cohen D 2005 *Solid State Commun.* **133** 583
[9] Thouless D J 1983 *Phys. Rev.* B **27** 6083
[10] Avron J E *et al* 1988 *Rev. Mod. Phys.* **60** 873
[11] Avron J E *et al* 2000 *Phys. Rev.* B **62** 618

[12] Cohen D, Kottos T and Schanz H 2005 *Phys. Rev.* E **71** 035202
[13] Reulet B, Ramin M, Bouchiat H and Mailly D 1995 *Phys. Rev. Lett.* **75** 124
[14] Bharucha C F, Robinson J C, Moore F L, Madison K W, Wilkinson S R, Sundaram B and Raizen M G 1997
         Atomic Physics vol 15 (Singapore: World Scientific) p 62
      Milner V, Hanssen J L, Campbell W C and Raizen M G 2001 *Phys. Rev. Lett.* **86** 1514
[15] Friedman N, Kaplan A, Carasso D and Davidson N 2001 *Phys. Rev. Lett.* **86** 1518
      Andersen M and Davidson N 2001 *Phys. Rev. Lett.* **87** 274101
[16] Bialynicki-Birula I and Bialynicka-Birula Z 1997 *Phys. Rev. Lett.* **78** 2539
[17] Sela I and Cohen D 2005 *Preprint* cond-mat/0512500
[18] Cohen D and Etzioni Y 2005 *J. Phys. A: Math. Gen.* **38** 9699
[19] Haake F 2001 *Quantum Signatures of Chaos* (Berlin: Springer)
[20] Brouwer P W and Beenakker C W J 1994 *Phys. Rev.* B **50** 11263
[21] Kottos T and Smilansky U 2003 *J. Phys. A: Math. Gen.* **36** 3501–24
[22] Wilkinson M and Austin E J 1993 *Phys. Rev.* A **47** 4
[23] Eckhardt B, Fishman S, Keating J, Agam O, Main J and Muller K 1995 *Phys. Rev.* E **52** 5893 and references
         therein
[24] Feingold M and Peres A 1986 *Phys. Rev.* A **34** 591
[25] Feingold M, Leitner D and Wilkinson M 1991 *Phys. Rev. Lett.* **66** 986